HHS Public Access

Author manuscript

J Magn Reson Imaging. Author manuscript; available in PMC 2023 October 01.

Quantitative MRI Differentiates Electromyography Severity Grades of Denervated Muscle in Neuropathy of the Brachial Plexus

Ek T. Tan, PhD[1], **Kenneth C. Serrano**[2], **Pravjit Bhatti**[3], **Farhad Pishgar, MD**[4], **Alyssa M. Vanderbeek**[1,5], **Carlo J. Milani, MD**[6], **Darryl B. Sneag, MD**[1]

[1]Department of Radiology and Imaging, Hospital for Special Surgery, New York, NY, USA 10021

[2]Renaissance School of Medicine at Stony Brook University, Stony Brook, NY, USA 11794

[3]Georgetown University School of Medicine, Washington DC, USA, 20007

[4]Russell H. Morgan Department of Radiology and Radiological Science, Johns Hopkins University School of Medicine, Baltimore, Maryland, USA, 21205

[5]Biostatistics Core, Research Administration, Hospital for Special Surgery, New York, NY, USA 10021

[6]Department of Physiatry, Hospital for Special Surgery, New York, NY, USA 10021

Abstract

Background: Quantitative MRI (qMRI) metrics reflect microstructural skeletal muscle changes secondary to denervation, and may correspond to conventional electromyography (EMG) assessments of motor unit recruitment (MUR) and denervation.

Hypothesis: Differences in quantitative T_2, diffusion-based apparent fiber diameter (AFD), and fat fraction (FF) exist between EMG grades, in patients with clinically suspected neuropathy of the brachial plexus.

Study Type: Prospective.

Population: 30 subjects (age=37.5±17.5, 21M/9F) with suspected brachial plexopathy.

Field Strength/Sequence: 3-Tesla; qMRI using fast spin echo (T_2-mapping), multi-b-valued diffusion-weighted echo planar imaging (for AFD) and dual-echo Dixon gradient echo (FF-mapping) sequences.

Assessment: qMRI values were compared against EMG grades (MUR and denervation). qMRI values (T_2, AFD and FF) were obtained for five regional shoulder muscles. A four-point scale was used for MUR/denervation severity.

Statistical tests: Linear mixed models and least-squares pairwise comparisons were used to evaluate qMRI differences between EMG grades. Predictive accuracy of EMG grades from

Corresponding Author:Ek T. Tan, PhD, Department of Radiology and Imaging, Hospital for Special Surgery, 535 E 70th Street, New York, NY 10021, USA, tane@hss.edu, Tel: +1(212)774-7601.

qMRI was quantified by ten-fold cross-validated logistic models. A p-value<0.05 was considered statistically significant.

Results: Mean (95% confidence interval) qMRI for 'full' MUR were T_2=39.40 msec (35.72–43.08 msec), AFD=78.35μm (72.52–84.19 μm) and FF=4.54% (2.11–6.97%). Significant T_2 increases (+8.36 to +14.67 msec) and significant AFD decreases (−11.04 to −21.58 μm) were observed with all abnormal MUR grades as compared to 'full' MUR. Significant changes in both T_2 and AFD were observed with increased denervation (+9.59 to +15.04 msec, −16.25 to −18.66 μm). There were significant differences in FF between some MUR grades (−1.45 to +2.96%), but no significant changes were observed with denervation (p=0.089–0.662). qMRI prediction of abnormal MUR or denervation was strong (mean accuracy= 0.841 and 0.810 respectively), but moderate at predicting individual grades (accuracy= 0.492 and 0.508 respectively).

Data Conclusion: Quantitative T_2 and AFD differences were observed between EMG grades in assessing muscle denervation.

Level of Evidence: 2

Technology Efficacy: Stage 1

Keywords

quantitative MRI; muscle denervation; neuropathy

INTRODUCTION

Peripheral nerve axonal injury results in muscle denervation(1). The 'reference standard' for assessing muscle denervation is needle electromyography (EMG)(2, 3), whereby the presence of fibrillation potentials (FPs) and/or positive sharp waves (PSWs) indicates active denervation(2). Denervation often results in reduced motor unit recruitment (MUR), also measured by EMG(2). Drawbacks of needle EMG are well-known, including its inherent invasiveness, limitations in probing deep-seated muscles, need to test muscles individually, and high operator-dependence(4). Furthermore, the onset of FPs can be variable (10 days to 4 weeks)(5), limiting EMG's use in the acute setting.

Brachial plexopathy, either traumatic or atraumatic (including inflammatory conditions) may result in sensorimotor disturbances and varying levels of impairment, depending on the severity of injury and segments involved(6)(7). Precise localization and assessment of injury extent may be complex(8), and a multidisciplinary approach comprising a physical exam, electrodiagnostic assessment (including EMG) (2), and imaging (MRI(7) and/or ultrasound) is routinely employed. MR neurography (MRN), or peripheral nerve MRI, provides a diagnostic adjunct to EMG to evaluate peripheral neuropathies(9). In MRN, T_2-weighted (T_2w), fat-suppressed sequences can simultaneously evaluate nerves and muscles(10). Of high relevance to MRI evaluation of brachial plexopathy are side- and terminal branch nerves arising from the plexus proper (roots to cords), including the suprascapular and axillary nerves innervating the rotator cuff muscles and thereby controlling to shoulder abduction and external rotation movements needed for daily activities.

Quantitative MRI can provide non-invasive information complementary to MRN, about the extent of muscle denervation in these critical muscles. In the denervated state, muscle T_2-prolongation results in part from increased extracellular fluid space(11), and manifests qualitatively as signal hyperintensity on T_2w images ('edema pattern')(12). MRI may be sensitive to early muscle denervation; following sciatic nerve transection in rats, T_2 value changes in muscle have been detected as early as 24 hours(13), and similar T_2w muscle signal changes have also been observed as early as 4 days following peripheral nerve injury in humans(14). In a preliminary study of subjects with muscle denervation, quantitative T_2-mapping provided superior ability to distinguish 'none' versus 'decreased' or 'discrete' MUR grades(15) as compared to qualitative T_2w imaging, using adjacent normal muscle T_2 as a reference. To detect muscle fatty infiltration observed in chronic neuropathies(14), low signal on fat-suppressed images may be utilized; quantitatively, elevated fat fraction (FF) in fat-water imaging more commonly-used in imaging of myopathies(16) may also apply to imaging chronic muscle denervation. Denervation also results in muscle atrophy(17), which may be depicted by diffusion tensor imaging (DTI)(18), as diffusion anisotropy increases with reduced muscle fiber diameter(19). Hence, multiparametric quantitative MRI (qMRI) may provide comprehensive muscle characterization. In EMG-tested denervated muscles with edema patterns on MRI, elevated T_2 and FF and decreased diffusion-based fiber diameters have been measured, as compared to muscles without edema patterns(20).

We hypothesized that T_2, muscle diameter, and FF differences would be observed between severity grades of denervation and MUR, and that there may be correlations between them. Therefore, the aim of this study was to determine if qMRI metrics could differentiate and predict EMG grades of denervation and MUR in patients with brachial plexopathies.

MATERIALS AND METHODS

Study Subjects

This prospective study was approved by our institutional review board with written subject consent and assent from all subjects was obtained.

A total of 38 subjects undergoing MRN for suspected brachial plexopathy, and who were also either scheduled to undergo electrodiagnostic testing including needle EMG or had a prior needle EMG report confirming the presence of muscle denervation were recruited consecutively between December 17, 2019 and March 19, 2021. The final number of subjects analyzed was n=30 (age=37.5±17.5, 21M/9F), and were scanned for various clinically suspected entities (Table 1). Parsonage-Turner syndrome accounted for most cases (17/30). Seven subjects were excluded due to the EMG performed outside of 50 days from the MRI, and one subject was ultimately not diagnosed with a peripheral neuropathy (Fig. 1).

Image Acquisition

A 10-minute, non-contrast-enhanced qMRI exam was added to routine unilateral brachial plexus MRI performed on one of two 3T MRI scanners with two 16-channel flexible receiver arrays (General Electric, Waukesha, WI, USA) positioned anterior and posterior to

the upper-chest-to-shoulder region. In addition to routine, fluid-sensitive (i.e. T_2-weighted) fat suppressed and proton-density weighted qualitative sequences(21) not analyzed in this work, qMRI scans including T_2-mapping (fast spin echo), multi-b-valued DTI (echo planar imaging) and fat fraction (FF)-mapping (dual-echo Dixon gradient echo) sequences (Table 2) were acquired. A recently developed apparent fiber diameter (AFD) metric described in detail in (20) using a cylindrical forward model(22) to depict the muscle fiber cross-section, was derived by mapping multi-b-valued DTI data to diameter values obtained using the forward model. As compared to radial diffusivity and fractional anisotropy, AFD relates directly to muscle fiber diameter, which readily lends itself for comparison to histology. To preclude the need for a normal muscle reference, correction of effects leading to spatially non-uniform maps was performed; namely, B_1+ correction was performed in a mono-exponential T_2-value computation(23) using B_1+ maps(24). Gradient nonlinearity correction in diffusion imaging was also performed to eliminate effects from spatial non-uniformity inherent to the gradient coil system(25). Echo planar imaging (EPI) distortion correction was performed on the scanner using vendor-provided software(26). FF calculations included estimated T_1 values of fat and muscle (without T_1-mapping)(27), primarily to reduce effects from T_1-bias, since high FF was not expected to characterize this patient cohort. Post-processing of multi-contrast data was performed on custom-written code in MATLAB (Mathworks Inc, Natick, MA, USA) to obtain T_2, AFD and FF maps, which were then converted to NIFTI volumetric format using DCM2NIIX(28). NIFTI data was registered using non-rigid image registration with Elastix(29), prior to manual segmentation on ITKSnap v3.8(30).

Observers and Image Evaluation

Regions of interests (ROIs) from five muscles (supraspinatus, infraspinatus, and deltoid anterior/middle/posterior heads) were manually segmented on three axial slices on the gradient echo image volume at the middle, upper and lower quadrant extent of each muscle. Segmentation was performed by two second-year medical student evaluators (KCS and PB), trained by a board-certified radiologist (DBS, 7 years of dedicated MR neurography experience). The supraspinatus muscle from 14 randomly selected slices were re-segmented by both evaluators after a one-month interval to determine the intra-rater Sørensen-Dice coefficient. EMG measures included 1) MUR (from maximal to least: ‘full’, ‘decreased, ‘discrete’ and ‘none’) and 2) abnormal spontaneous activity indicating denervation severity (FPs and PSWs) (of increasing abnormality: ‘0’, ‘1+’, ‘2+’, ‘3+’, ‘4+’), according to standard practice (31). Generally, ‘full’ MUR occurred when there was complete motor unit activation and the EMG screen was entirely filled. ‘Decreased’ MUR occurred when the entire EMG screen was not filled, but greater than 3 motor units were identified. ‘Discrete’ MUR showed a maximum of 1–3 motor units firing during maximum effort. For denervation, ‘0’ was the absence of FPs or PSWs, ‘1+’ was persistent/unsustained single trains in at least 1 muscle region, ‘2+’ was moderate numbers in 2 or more muscle areas, ‘3+’ was many trains in all muscle regions, ‘4+’ was an obliteration of the baseline with PSWs and FPs in all areas of muscle examined. EMG reports from nine different operators (average 21.6 years, range 6–35 years’ experience, including CJM) were reviewed. As some EMG reports listed abnormal spontaneous activity as either FPs or PSWs and others listed

both, only the more severe of the two measurements was considered for analysis, as both measures are considered to reflect denervation(32).

Statistical Analysis

Linear mixed models were utilized to assess differences in MRI metrics (T_2, AFD, or FF) across EMG grades (MUR, or FP/PSW), accounting for multiple muscle ROI measurements per subject. Marginal means and confidence intervals for MRI measures across EMG grades were reported. Least-squares pairwise comparisons for MRI measures across EMG grades used Benjamini-Hochberg correction(33) to reduce the false discovery rate, with $p<0.05$ deemed statistically significant. To determine correlation between continuous (MRI) and ordinal (EMG) variables, Kendall's τ was applied between each MRI metric and EMG grade (0 to ±0.19: negligible, ±0.2 to ±0.39: weak, ±0.4 to ±0.59: moderate, ±0.6 to ±0.79: strong, ±0.8 to ±1.0: near perfect). To determine the predictive value of MRI measures for EMG grades, multivariable logistic models were used to separately assess both binary and four-point-scale predictions of abnormal MUR and denervation (no '4+' were observed), with 10-fold repeated cross-fold validation and up-sampling. Overall accuracy was reported with 95% confidence intervals.

Inter-rater Sørensen-Dice coefficients were computed to determine the extent of ROI overlap between both segmentation evaluators. In addition, inter-rater segmentation repeatability was determined by performing paired t-tests between MRI measures from both evaluators. Analysis was performed using R version 4.0.3 (R Foundation).

RESULTS

Of the 150 possible muscle ROIs from n=30 subjects with neuropathy, 127 ROIs were drawn as some muscles were either not tested by EMG (n=22) or inadvertently excluded from the field-of-view on the qMRI scans (n=1). Of these 127 muscle ROIs, 89 were abnormal and 38 were normal with normalcy defined by either 'decreased' or worse MUR or '1+' or greater denervation. Most subjects (n=28) had ≥1 abnormal muscle ROIs (Fig. 2); the other two subjects were diagnosed with muscle denervation, but EMG was not performed on the denervated muscles. Neuropathies involved either the suprascapular nerve (innervating the supraspinatus and infraspinatus muscles) (Fig. 3), the axillary nerve (deltoid muscle) (Fig. 4) or both.

MUR Severity Grades

T_2 was observed to increase monotonically with lower MUR (Fig. 5a, Table 3). Almost all paired comparisons showed significantly higher T_2 with lower MUR (Table 4). As compared to 'full' MUR (mean-T_2=39.40 msec), mean-T_2 was significantly higher in 'decreased' (47.77 msec), 'discrete' (53.39 msec) and 'none' (54.07 msec). Significantly higher mean-T_2 was also observed in 'discrete' (by +5.62 msec) and 'none' (by +6.30 msec) relative to 'decreased'. Mean-T_2 of 'none' and 'discrete' were not significantly different (p=0.7185).

AFD was observed to decrease monotonically with lower MUR, with most paired comparisons showing statistically significantly lower AFD with lower MUR. Compared to 'full' (78.35 μm), mean-AFD was significantly lower in 'decreased' (67.30 μm), 'discrete'

(59.44 μm), and ‘none’ (56.77μm). ‘None’ MUR had significantly lower mean-AFD than ‘decreased’ (by −10.53 μm). Comparisons of ‘discrete’ vs ‘decreased’ and ‘none’ vs ‘discrete’ were not statistically significant (p=0.0990 and 0.4392, respectively).

FF was mostly increased with lower MUR. Mean-FF was significantly higher in ‘discrete’ (7.46%) and ‘none’ (6.00%) as compared to ‘full’ (4.54%). Mean-FF was also significantly higher in ‘discrete’ than ‘decreased’ (by 2.56%). However, mean-FF was significantly lower in ‘none’ than ‘discrete’ (−1.45%). Comparisons of ‘decreased’ vs. ‘none’ and ‘full’ were not statistically significant (p=0.216 and 0.608, respectively).

FP/PSW

T_2 values demonstrated an increasing trend with denervation severity (i.e. FP/PSW) (Fig. 5b, Table 3). Significantly higher mean-T_2 was observed in all denervated states (by +9.59 to +15.05 msec) as compared to ‘0’ (40.69 msec). Mean-T_2 was significantly higher in ‘3+’ than ‘2+’ (by +5.44 msec). AFD decreased with denervation. Significantly lower mean-AFD was observed in ‘2+’ (58.93μm) and ‘3+’ (56.52 μm) than in ‘0’ (75.18 μm). AFD in ‘3+’ was significantly lower than that in ‘1+’ (by −13.85 μm). No significant differences in fat fraction were observed among different muscle denervation grades (p=0.089 to 0.662).

Correlations and Prediction of EMG from qMRI

All correlation analyses were statistically significant; correlation was moderate between T_2 and MUR (τ=0.549) and between T_2 and denervation, (τ=0.438). Correlation was moderate between AFD and MUR (τ=−0.441), but weak between AFD and MUR (τ=−0.203). Correlation was weak between FF and MUR (τ=0.296), and negligible between FF and denervation (τ=0.120).

qMRI measures were strongly predictive in binary prediction of abnormal MUR (‘decreased’, ‘discrete’, ‘none’) vs normal (‘full’) muscles (accuracy=0.841) (Table 5). Prediction for individual MUR grades was moderate (accuracy=0.492). The results for denervation (abnormal FP/PSW) were similar, with strong binary prediction (‘1+’ and above vs ‘0’ with accuracy=0.810), and moderate prediction for individual denervation grades (accuracy= 0.508).

Inter-rater Segmentation Repeatability

The inter-rater mean Sørensen-Dice coefficient across all ROIs was 0.828 (standard deviation: 0.119), and resulting differences in quantitative parameters were small (mean T_2: −0.420 ms, p=0.0997, AFD: +0.223 μm, p=0.632, FF: +0.159%, p=0.431), and not statistically significantly different. The intra-rater Sørensen-Dice score of 0.844 (standard deviation: 0.120) was similar to the inter-rater Sørensen-Dice score.

DISCUSSION

Changes in qMRI metrics were observed between EMG grades of MUR and denervation in denervated muscles innervated by the brachial plexus. Specifically, T_2 increases and AFD decreases were observed to correlate with lower MUR, with most comparisons between

grades shown to be significant. While the current T_2 results parallel previous findings(15), AFD and FF may provide additional characterization of atrophy and fat infiltration. Also, the bias corrections for T_2 and diffusion used here obviated the need for a normal muscle reference that may be unavailable for analysis.

qMRI metrics provide objective information regarding muscle denervation status that is complementary to electrodiagnostic and MRN exams in the evaluation of brachial plexopathy. In our current practice, electrodiagnostic exams often precede MRN, to inform on the relevant imaged anatomy. As the qMRI protocol employed in this study requires a total of 10 minutes, and can be readily appended to an MRN exam, knowledge of MRN and qMRI results preceding an electrodiagnostic exam may alternatively inform on muscles required for testing with needle EMG.

While fatty infiltration is thought to occur chronically (>6 months), the extent of fatty infiltration may vary depending on the etiology of the neuropathy(34, 35). This study did not include sufficient subjects to study chronically denervated muscles, as only 8/30 subjects were studied >6 months from symptom onset, and most denervated muscles had low FF (<10%). Furthermore, an overlap in FF distribution between chronic (2.7–40%) and non-chronic cases (0.8–13%) was observed. Consequently, we observed mixed trends of increased FF with lower MUR at small effect sizes, and no significant FF changes with denervation. Specifically, the ‘1+’ denervation FF values were biased high because 4/14 muscle ROIs came from one subject with chronic muscle denervation.

This study demonstrated that MRI provided strong predictive ability based on a binary classification of both MUR and denervation, and moderate overall prediction on a four-point grading scheme. However, this study was not powered for prediction, and results may be improved with a larger homogenous patient cohort, and with the addition of qualitative or quantitative nerve evaluation. These predictions mirror the paired comparison results, where large significant differences in T_2 and AFD values were seen for ‘full’ vs all abnormal MUR grades, but less so between individual abnormal MUR grades. Importantly, pre-operative tests (EMG or qMRI) separating intermediate MUR grades of ‘decreased’ from ‘discrete’ may have prognostic value in predicting success of nerve transfer surgeries (36). In this study, we found a significant difference in T_2 between these MUR grades. As such, qMRI may provide valuable information as an operator-independent and non-invasive means for qualifying muscle denervation, complementary to conventional, qualitative MRI and EMG.

T_2 and AFD differences, while significant, did not correlate as strongly with denervation grades. Aside from variability due to qMRI, variability in operator experience, location of needle placement from nine EMG operators, heterogeneity in disease type, onset and severity may also have contributed to variability in these findings. Specifically, subjects with denervated muscle may have neither abnormal fibrillations nor PSWs despite severely reduced MUR and high T_2, due to chronicity (>6 months). This study did not attempt to exclude such measurements from analysis (11 muscle ROIs), to ensure generalizability of results to patients who may present to MRI without a specific disease type or with uncertain time course.

Correlations between T_2, AFD and FF have previously been reported(20, 37). To analyze the effects from fat on T_2, a linear signal (S) equation could be used in the form of $S = FFe^{-TE/T2M} + (1 - FF)e^{-TE/T2F}$, where T_2 of fat/muscle may respectively be assumed to be T_{2F}=130 msec and T_{2M}=35 msec at 3-Tesla. At an average TE=40 msec in this work, a 3% increase in fat fraction would result in a ~1.3 msec increase in T_2. This implies that any fat fraction increase observed between EMG grades, maximally ~3% in this work, contributes negligibly to the increase in T_2. Increased fat correlates with increased diffusion fractional anisotropy(37), which in turn can negatively bias AFD. Nevertheless, this study analyzed qMRI metrics independently. To strengthen conclusions from this study, the Benjamini-Hochberg correction(33) was adopted over other multiple-comparison methods to reduce discovery of false negatives as well as false positives.

Future Work

This study cohort included eight subjects from the first time-point of an on-going longitudinal study on Parsonage Turner syndrome (PTS). Future work would include longitudinal analysis of this PTS cohort and expand analysis to other muscles involved. While the recently developed AFD metric shows promise for evaluating muscle denervation and provides superior sensitivity relative to conventional diffusion measures(20), it has yet to be validated with histology. Future work would include validation of AFD against ex vivo microscopic diameter assessment of muscle biopsy samples.

Limitations

This study did not include a homogeneous disease cohort or baseline (at time of symptom onset) scans, which could help confirm if muscle T_2 increases and AFD decreases were due solely to neuropathy. This study did not utilize a common normal muscle reference, which could be helpful if spatial correction methods were unavailable. For the shoulder region, the subscapularis muscle could be chosen as a reference, but EMG is not typically performed on this deep-seated muscle. Data of provider-reported muscle strength of shoulder abduction and external rotation were available, but correlations against MRI were not analyzed as muscle strength testing is often unable to isolate individual muscles (e.g. deltoid vs. supraspinatus) and in particular individual deltoid muscle heads.

Baseline imaging could also be useful to account for inter-subject variation in qMRI, especially AFD, since population variation of muscle fiber diameter is well reported(17). Serial imaging data was not included, which could facilitate analysis of longitudinal changes of MRI with EMG to depict either disease progression or recovery. This findings of this study, in particular for predicting EMG with MRI, were also limited by the relatively small sample size (n=30).

Conclusion

Quantitative T_2 and AFD changes may complement EMG as an operator-independent and non-invasive means for assessing muscle denervation.

ACKNOWLEDGEMENTS

The authors will like to thank Joseph Feinberg for sharing his expertise on EMG. We also thank Sophie Queler and Emily Pedrick for assistance with patient recruitment, and Maggie Fung, Yan Wen and Jaemin Shin with pulse sequence development assistance.

Funding Support

National Institute of Health (NIH) National Center for Advancing Translational Sciences (NCATS) R21TR003033

REFERENCES

1. Sunderland S: A Classification Of Peripheral Nerve Injuries Producing Loss Of Function. Brain 1951; 74:491–516. [PubMed: 14895767]
2. Feinberg J: EMG: Myths and Facts. Hss J 2006; 2:19–21. [PubMed: 18751841]
3. Chaudhry V, Cornblath DR: Wallerian degeneration in human nerves: Serial electrophysiological studies. Muscle Nerve 1992; 15:687–693. [PubMed: 1324426]
4. Narayanaswami P, Geisbush T, Jones L, et al. : Critically re-evaluating a common technique. Neurology 2016; 86:218–223. [PubMed: 26701380]
5. Willmott AD, White C, Dukelow SP: Fibrillation potential onset in peripheral nerve injury. Muscle Nerve 2012; 46:332–340. [PubMed: 22907222]
6. Tharin BD, Kini JA, York GE, Ritter JL: Brachial Plexopathy: A Review of Traumatic and Nontraumatic Causes. Am J Roentgenol 2014; 202:W67–W75. [PubMed: 24370167]
7. Sneag DB, Rancy SK, Wolfe SW, et al. : Brachial plexitis or neuritis? MRI features of lesion distribution in Parsonage–Turner syndrome. Muscle Nerve 2018; 58:359 366. [PubMed: 29461642]
8. Rubin DI: Brachial and lumbosacral plexopathies: A review. Clin Neurophysiology Pract 2020; 5:173–193.
9. Lisle D, Johnstone S: Usefulness of muscle denervation as an MRI sign of peripheral nerve pathology. Australas Radiol 2007; 51:516–526. [PubMed: 17958685]
10. Sneag DB, Queler S: Technological Advancements in Magnetic Resonance Neurography. Curr Neurol Neurosci 2019; 19:75.
11. Polak JF, Jolesz FA, Adams DF: Magnetic Resonance Imaging of Skeletal Muscle Prolongation of T1 and T2 Subsequent to Denervation. Invest Radiol 1988; 23:365–369. [PubMed: 3384617]
12. Kim S-J, Hong SH, Jun WS, et al. : MR Imaging Mapping of Skeletal Muscle Denervation in Entrapment and Compressive Neuropathies. Radiographics 2011; 31:319–332. [PubMed: 21415181]
13. Bendszus M, Koltzenburg M, Wessig C, Solymosi L: Sequential MR imaging of denervated muscle: experimental study. Ajnr Am J Neuroradiol 2002; 23:1427–31. [PubMed: 12223392]
14. West GA, Haynor DR, Goodkin R, et al. : Magnetic Resonance Imaging Signal Changes in Denervated Muscles after Peripheral Nerve Injury. Neurosurgery 1994; 35:1077–1086. [PubMed: 7885552]
15. Argentieri EC, Tan ET, Whang JS, et al. : Quantitative T2-mapping magnetic resonance imaging for assessment of muscle motor unit recruitment patterns. Muscle Nerve 2021; 63:703–709. [PubMed: 33501678]
16. Sinclair CDJ, Morrow JM, Janiczek RL, et al. : Stability and sensitivity of water T2 obtained with IDEAL-CPMG in healthy and fat-infiltrated skeletal muscle. Nmr Biomed 2016; 29:1800–1812. [PubMed: 27809381]
17. Maier F, Bornemann A: Comparison of the muscle fiber diameter and satellite cell frequency in human muscle biopsies. Muscle Nerve 1999; 22:578–583. [PubMed: 10331356]
18. Holl N, Echaniz-Laguna A, Bierry G, et al. : Diffusion-weighted MRI of denervated muscle: a clinical and experimental study. Skeletal Radiol 2008; 37:1111–1117. [PubMed: 18682930]
19. Berry DB, Regner B, Galinsky V, Ward SR, Frank LR: Relationships between tissue microstructure and the diffusion tensor in simulated skeletal muscle. Magnet Reson Med 2018; 80:317–329.

20. Tan ET, Zochowski KC, Sneag DB: Diffusion MRI fiber diameter for muscle denervation assessment. Quantitative Imaging Medicine Surg 2021; 0:0–0.
21. Sneag DB, Zochowski KC, Tan ET: MR Neurography of Peripheral Nerve Injury in the Presence of Orthopedic Hardware: Technical Considerations. Radiology 2021; 300:246–259. [PubMed: 34184933]
22. Neuman CH: Spin echo of spins diffusing in a bounded medium. J Chem Phys 1974; 60:4508 4511.
23. Sumpf TJ, Petrovic A, Uecker M, Knoll F, Frahm J: Fast T2 Mapping with Improved Accuracy Using Undersampled Spin-Echo MRI and Model-Based Reconstructions with a Generating Function. Ieee T Med Imaging 2014; 33:2213–2222.
24. Sacolick LI, Wiesinger F, Hancu I, Vogel MW: B1 mapping by Bloch-Siegert shift. Magnet Reson Med 2010; 63:1315–1322.
25. Tan ET, Marinelli L, Slavens ZW, King KF, Hardy CJ: Improved correction for gradient nonlinearity effects in diffusion-weighted imaging. J Magn Reson Imaging 2012; 38:448–53. [PubMed: 23172675]
26. Hancu I, Lee S-K, Hulsey K, et al. : Distortion correction in diffusion-weighted imaging of the breast: Performance assessment of prospective, retrospective, and combined (prospective + retrospective) approaches. Magnet Reson Med 2017; 78:247 253.
27. Liu C, McKenzie CA, Yu H, Brittain JH, Reeder SB: Fat quantification with IDEAL gradient echo imaging: Correction of bias from T1 and noise. Magnet Reson Med 2007; 58:354–364.
28. Li X, Morgan PS, Ashburner J, Smith J, Rorden C: The first step for neuroimaging data analysis: DICOM to NIfTI conversion. J Neurosci Meth 2016; 264:47–56.
29. Klein S, Staring M, Murphy K, Viergever MA, Pluim JPW: elastix: a toolbox for intensity-based medical image registration. Ieee T Med Imaging 2010; 29:196 205.
30. Yushkevich PA, Piven J, Hazlett HC, et al. : User-guided 3D active contour segmentation of anatomical structures: Significantly improved efficiency and reliability. Neuroimage 2006; 31:1116–1128. [PubMed: 16545965]
31. Schreiber JJ, Feinberg JH, Byun DJ, Lee SK, Wolfe SW: Preoperative Donor Nerve Electromyography as a Predictor of Nerve Transfer Outcomes. J Hand Surg 2014; 39:42–49.
32. Willmott AD, White C, Dukelow SP: Fibrillation potential onset in peripheral nerve injury. Muscle Nerve 2012; 46:332–340. [PubMed: 22907222]
33. Benjamini Y, Hochberg Y: Controlling the False Discovery Rate: A Practical and Powerful Approach to Multiple Testing. J Royal Statistical Soc Ser B Methodol 1995; 57:289–300.
34. Scalf RE, Wenger DE, Frick MA, Mandrekar JN, Adkins MC: MRI Findings of 26 Patients with Parsonage-Turner Syndrome. Am J Roentgenol 2007; 189:W39–W44. [PubMed: 17579134]
35. Kamath S, Venkatanarasimha N, Walsh MA, Hughes PM: MRI appearance of muscle denervation. Skeletal Radiol 2008; 37:397–404. [PubMed: 18360752]
36. Schreiber JJ, Feinberg JH, Byun DJ, Lee SK, Wolfe SW: Preoperative Donor Nerve Electromyography as a Predictor of Nerve Transfer Outcomes. J Hand Surg 2014; 39:42–49.
37. Williams SE, Heemskerk AM, Welch EB, Li K, Damon BM, Park JH: Quantitative effects of inclusion of fat on muscle diffusion tensor MRI measurements. J Magn Reson Imaging 2013; 38:1292 1297.References>

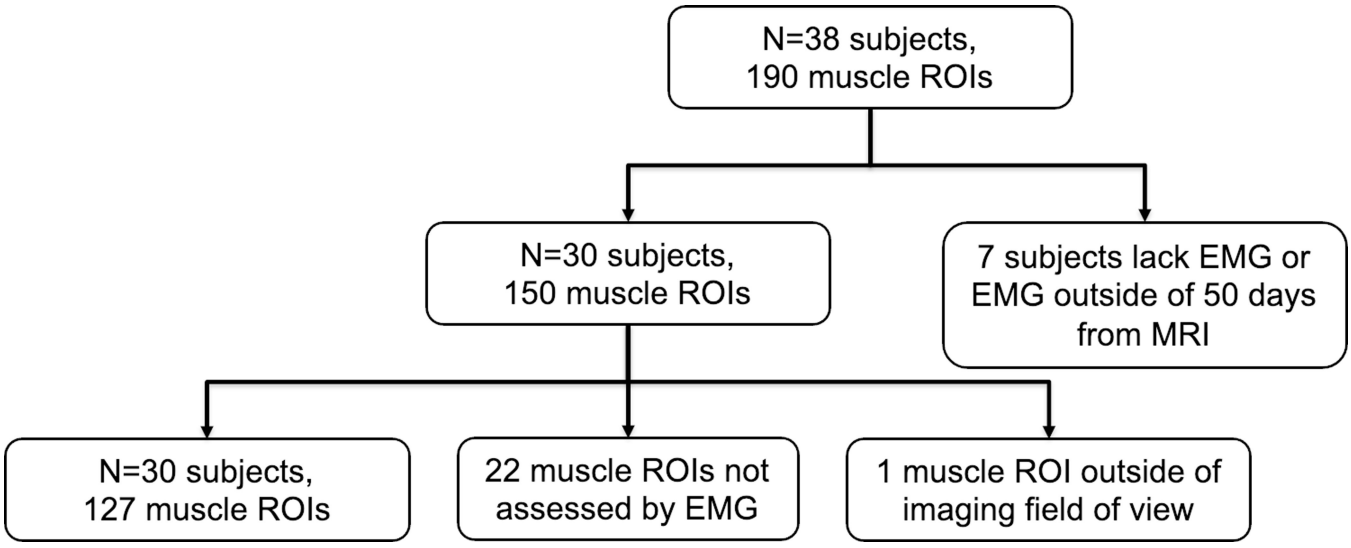

Figure 1.
Flow diagram for subject and muscle ROI inclusion for analysis.

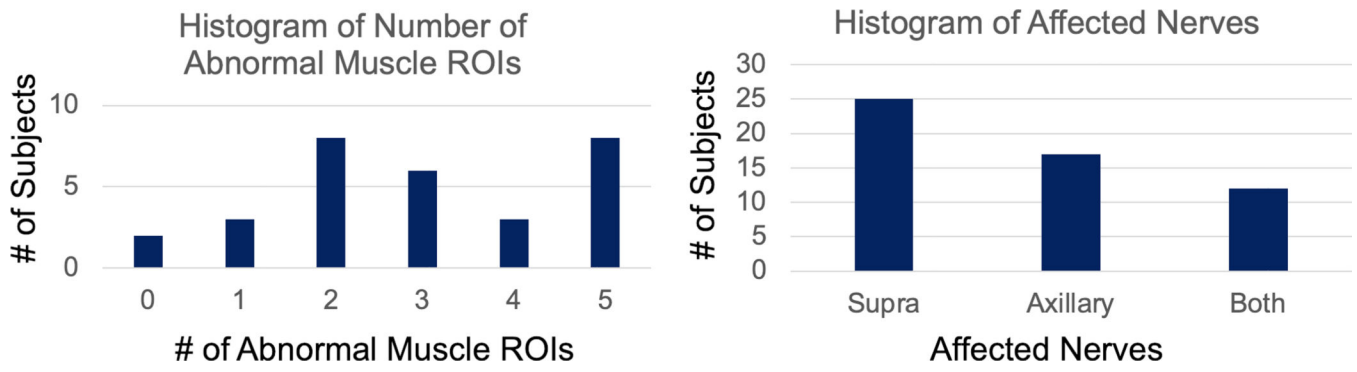

Figure 2.

Histograms of subjects by (a) number of abnormal muscle ROIs (reduced MUR or presence of denervation potentials on EMG), and (b) involvement of either or both the suprascapular and axillary nerves.

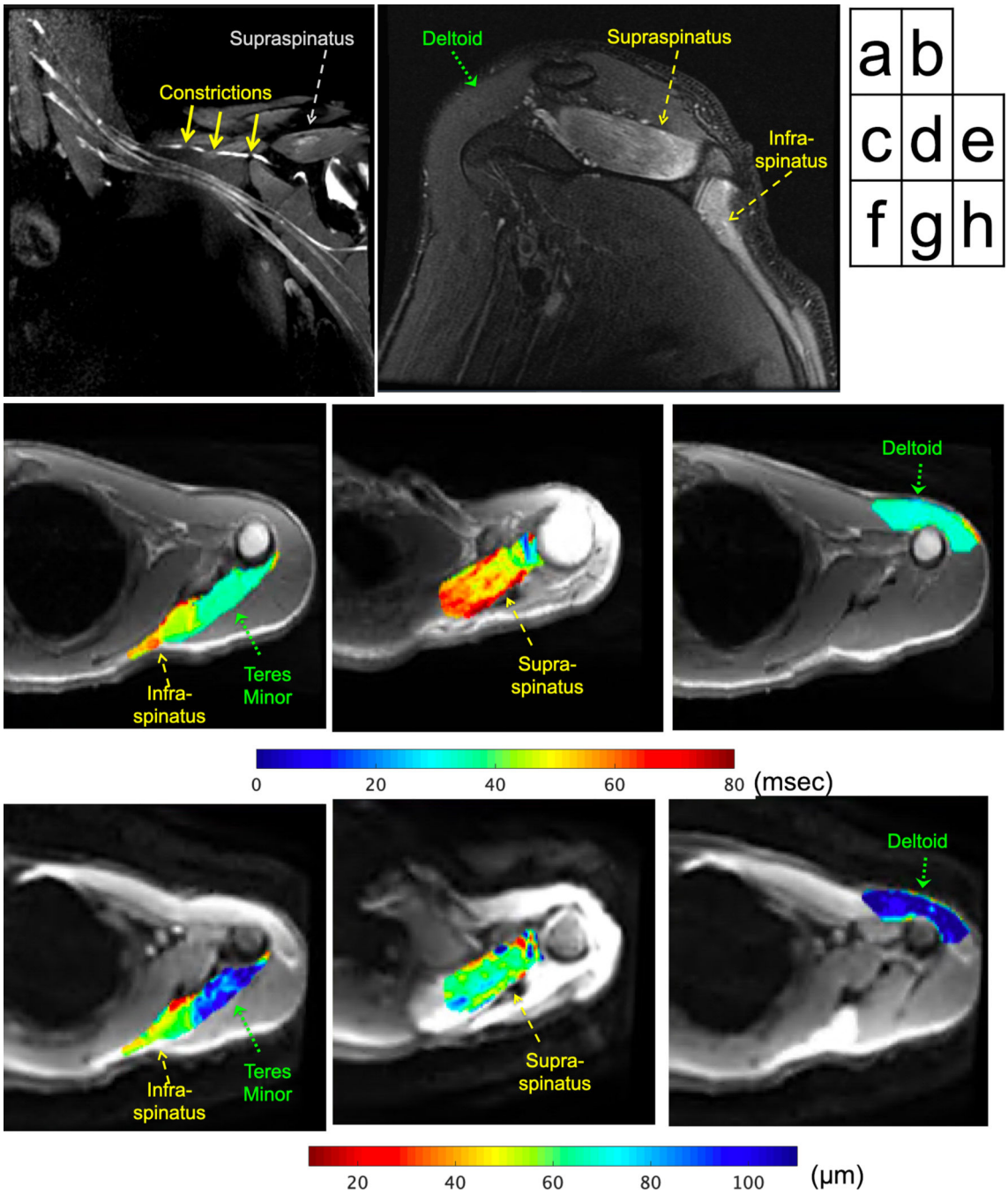

Figure 3.

22 year-old male subject with left shoulder abduction and external rotation weakness, diagnosed with Parsonage-Turner syndrome. MRI three months post symptom onset shows (a) three severe constrictions (solid arrows) of the suprascapular nerve on the post-contrast, coronal 3D FSE maximum intensity projection. Edema patterns of the supraspinatus/infraspinatus muscles are seen on the (b) oblique-sagittal FSE image (note normal deltoid). Quantitative, axial T_2 maps (overlaid on magnitude T_2w) show (c) higher T_2 in infraspinatus (MUR: 'none', fibrillations: '3+') adjacent to lower T_2 non-denervated teres minor (not

assessed by EMG), (d) higher T_2 in supraspinatus (MUR: ‘discrete’, FP: ‘2+’), and (e) lower T_2 in anterior deltoid (MUR: ‘full’, FP/PSW: ‘0’). Apparent fiber diameter (AFD) maps (overlaid on trace diffusion magnitude) corresponding to axial locations show (f) lower AFD in infraspinatus, higher AFD in teres minor, (g) lower AFD in supraspinatus, and (h) higher AFD in the deltoid.

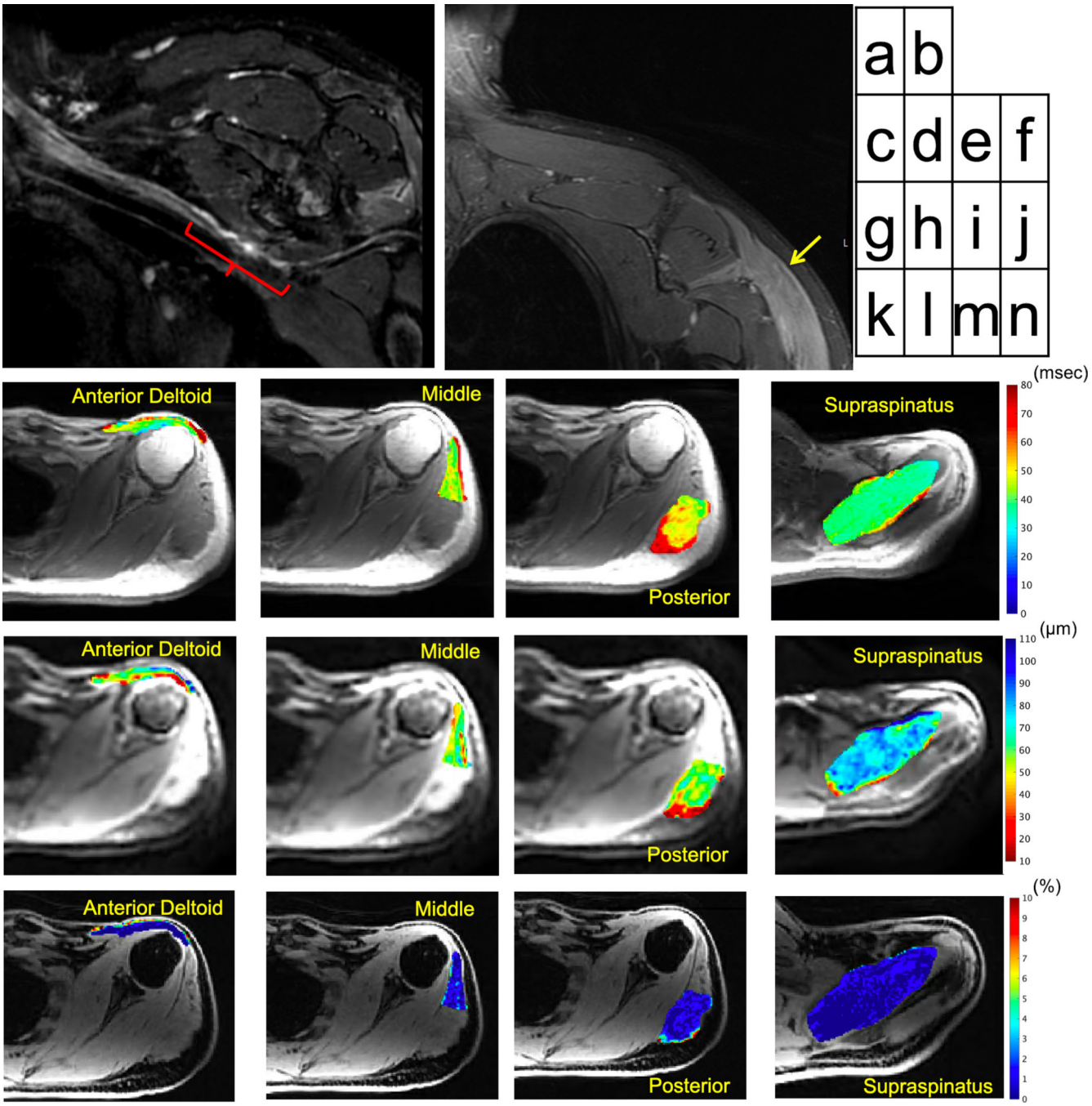

Figure 4.

44 year-old male with neuropathy of the left axillary neuropathy following Bankart repair. MRI six months post surgery shows (a) segmental thickening and irregular morphology of the axillary nerve (red bracket) as it courses inferior to the subscapularis muscle on the coronal 3D inversion-recovery FSE image (curved multiplanar reformat), and (b) denervated deltoid muscle (arrow) on the coronal 2D Dixon-water FSE image. Quantitative axial T_2-maps (in msec) show mildly increased T_2 in (c) anterior (MUR: 'none', FP/PSW: '2+'), (d) middle (MUR: 'discrete', FP/PSW: '2+') and (e) posterior deltoid heads (MUR:

‘discrete’, FP/PSW: ‘2+’) in part due to mild fatty infiltration, relative to (f) lower T_2 on normal supraspinatus (MUR: ‘full’, FP/PSW: ‘0’). Corresponding axial apparent fiber diameter (AFD) maps (in μm) show (g-i) lower AFD in the deltoid, and (j) higher AFD in supraspinatus. Fat fraction (k-n) was low in all muscles (in %).

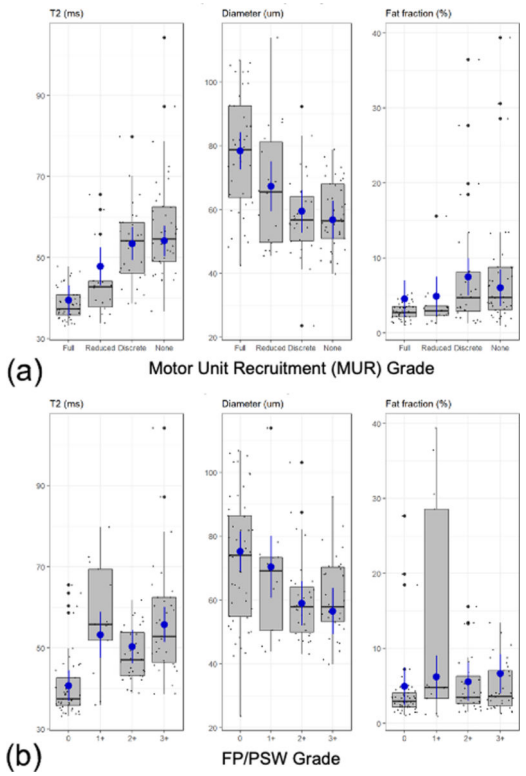

Figure 5.

Box-plots and marginal mean estimates (blue) of MRI measures (T_2, apparent fiber diameter, and fat fraction) with respect to EMG grades of (a) MUR and (b) FP/PSW.

Table 1.

Summary of demographics and indications for patients with both EMG and brachial plexus MRI

Demographics				
	Male/Female	21 / 9		
	Age, (mean/SD)	37.5 / 17.5		
	Left/Right	15 / 15		
	Days between EMG and MRI (mean/median)	11.2/6.5		
	Days from symptom onset to EMG (mean/median)	290/87		
	Days from symptom onset to MRI (mean/median)	301/90		
Indications				
	Indication	**Number of Subjects**		
	PTS	17		
	Traumatic brachial plexopathy	6		
	Atraumatic brachial plexopathy of unknown cause	4		
	Iatrogenic injury (previous shoulder surgery)	1		
	Post-radiation brachial plexopathy	1		
	ALS	1		
Muscle ROIs				
	Muscle ROI	**Abnormal**	**Normal**	**Not Assessed by EMG**
	Supraspinatus	17	3	9
	Infraspinatus	22	2	6
	Anterior Deltoid	17	10	3
	Middle Deltoid	18	12	0
	Posterior Deltoid	15	11	4
	Total	**89**	**38**	**22**

EMG: Electromyography, PTS: Parsonage Turner syndrome, ALS: amyotrophic lateral sclerosis, ROI: region of interest, SD: standard deviation

Table 2.

Imaging parameters of quantitative MRI protocol.

Sequence	T_2-mapping 2D T_2w-FSE	2D Multi-shell DTI-EPI	3D, 2-echo Dixon GRE	2D B_1+ mapping
Scan time (min:sec)	4:12	4:56	0:48	0:44
Orientation	Axial	Axial	Axial	Axial
Field-of-view (FOV) (cm)	27.0	27.0	34.0	27.0
TR/TE (ms)	2400/10–80	3300/56	4.2/1.2, 2.5	11/7
Matrix size (frequency x phase)	192 × 128	90 × 90	256 × 256	64 × 64
Phase FOV factor	1.50	-	-	-
Slice thickness (mm), Spacing	4.0, 1.0	3.0, -	1.8, -	5.0, -
Slices	26	35	96	26
Bandwidth (kHz)	±15.6	±250.0	±142.9	±15.6
Echo train length	8	51	2	-
Parallel imaging factor (phase)	2	1.5	1.5	-
GRE Flip Angle (°)	-	-	10	10
b-values (s/mm^2) [# directions]	-	0 [2] 375 [13] 750 [27] [Total=40]	-	-
Fat suppression method	None	Spectral-spatial pulse	Dixon	None

FSE: fast/turbo spin echo, DTI: diffusion tensor imaging, GRE: gradient recalled echo, TR: repetition time, TE: echo time

Table 3:

Marginal mean estimates (and 95% confidence intervals) for T_2, AFD, and FF across MUR and FP/PSW grades. The number of muscles included is given for each grade.

	T_2 (msec)	AFD (μm)	FF (%)
MUR			
Full (n=41)	39.40 (35.72, 43.08)	78.35 (72.52, 84.19)	4.54 (2.11, 6.97)
Reduced (n=18)	47.77 (43.09, 52.45)	67.30 (59.49, 75.12)	4.90 (2.30, 7.50)
Discrete (n=27)	53.39 (49.31, 57.46)	59.44 (52.79, 66.08)	7.46 (4.97, 9.95)
None (n=41)	54.07 (50.29, 57.86)	56.77 (50.80, 62.75)	6.00 (3.56, 8.45)
FP/PSW			
0 (n=49)	40.69 (36.90, 44.48)	75.18 (68.92, 81.44)	4.94 (2.44, 7.44)
1+ (n=14)	53.23 (47.55, 58.91)	70.38 (60.66, 80.09)	6.18 (3.31, 9.06)
2+ (n=31)	50.29 (46.13, 54.45)	58.93 (51.93, 65.93)	5.56 (3.00, 8.12)
3+ (n=34)	55.74 (51.42, 60.05)	56.52 (49.30, 63.74)	6.61 (4.02, 9.20)
4+ (n=0)	-	-	-

AFD: apparent fiber diameter, FF: fat fraction, EMG: electromyography, MUR: motor unit recruitment, FP/PSW: fibrillation potentials/positive sharp waves

Table 4:

Linear least-squares pairwise comparisons for T_2, AFD, and FF across MUR and FP/PSW grades. Positive values indicate the first group had a larger average than the second group. P-values used a Benjamin-Hochberg correction for multiple comparison, whereby p<0.05 was considered statistically significant.

	Comparison	Difference	95% CI	p-value
MUR	**T2 (msec)**			
	Decreased - Full	+8.36	+4.05, +12.68	0.0005**
	Discrete - Full	+13.98	+10.10, +17.87	<0.0001***
	None - Full	+14.67	+11.12, +18.22	<0.0001***
	Discrete - Decreased	+5.62	+0.75, +10.49	0.0305*
	None - Decreased	+6.30	+1.40, +11.21	0.0197*
	None - Discrete	+0.68	−3.03, +4.40	0.7185
	AFD (μm)			
	Decreased - Full	−11.04	−18.92, −3.18	0.0136*
	Discrete - Full	−18.91	−26.01, −11.82	<0.0001***
	None - Full	−21.58	−28.01, −15.15	<0.0001***
	Discrete - Decreased	−7.86	−16.68, +0.94	0.0990
	None - Decreased	−10.53	−19.29, −1.77	0.0301*
	None - Discrete	−2.66	−9.39, +4.06	0.4392
	FF (%)			
	Decreased - Full	+0.036	−1.01, +1.74	0.6080
	Discrete - Full	+2.92	+1.70, +4.15,	0.0001**
	None - Full	+1.46	+0.34, +2.60	0.0238*
	Discrete - Decreased	+2.56	+1.00, +4.13	0.0054*
	None - Decreased	+1.10	−0.50, +2.71	0.2160
	None - Discrete	−1.45	−2.62, −0.29	0.0238*
FP/PSW	**T2 (msec)**			
	‘1+’ – ‘0’	+12.54	+7.06, +18.02	<0.0001***
	‘2+’ – ‘0’	+9.59	+6.06, +13.13	<0.0001***
	‘3+’ – ‘0’	+15.04	+11.11, +18.99	<0.0001***
	‘2+’ – ‘1+’	−2.94	−8.82, +2.93	0.3912
	‘3+’ – ‘1+’	+2.50	−3.20, +8.20	0.3912
	‘3+’ – ‘2+’	+5.44	+1.12, +9.77	0.0226*
	AFD (μm)			
	‘1+’ – ‘0’	−4.80	−14.54, +4.93	0.4023

	Comparison	Difference	95% CI	p-value
	‘2+’ – ‘0’	−16.25	−22.75, −9.75	<0.0001***
	‘3+’ – ‘0’	−18.66	−25.80, −11.53	<0.0001***
	‘2+’ – ‘1+’	−11.44	−21.88, −1.01	0.0503
	‘3+’ – ‘1+’	−13.85	−23.78, −3.94	0.0142*
	‘3+’ – ‘2+’	−2.41	−10.26, +5.44	0.5479
	FF (%)			
	‘1+’ – ‘0’	+1.23	−0.64, +3.11	0.3969
	‘2+’ – ‘0’	+0.61	−0.55, +1.78	0.4564
	‘3+’ – ‘0’	+1.67	+0.35, +2.99	0.0891
	‘2+’ – ‘1+’	−0.622	−2.64, +1.39	0.6551
	‘3+’ – ‘1+’	+0.43	−1.50, +2.36	0.6623
	‘3+’ – ‘2+’	+1.05	−0.40, +2.51	0.3969

*<0.05

**<0.005

***<0.0001

AFD: apparent fiber diameter, FF: fat fraction, EMG: electromyography, MUR: motor unit recruitment, FP/PSW: fibrillation potentials/positive sharp waves

Table 5:

Overall accuracy (95% CI) of qMRI measures to predict EMG grades.

	Measure type	Overall Accuracy (95% CI)
MUR	**Binary ('Full' vs all others)**	0.841 (0.766, 0.900)
	All grades	0.492 (0.402, 0.583)
FP/PSW	**Binary ('0' vs all others)**	0.810 (0.730, 0.874)
	All grades	0.508 (0.417, 0.598)